International Journal of Chemical, Materials and Biomolecular Sciences
ISSN: 2415-6620
Vol:12, No:3, 2018

Single-Walled Carbon Nanotube Synthesis by Chemical Vapor Deposition Using Platinum-Group Metal Catalysts

T. Maruyama, T. Saida, S. Naritsuka, S. Iijima

***Abstract*—**Single-walled carbon nanotubes (SWCNTs) are generally synthesized by chemical vapor deposition (CVD) using Fe, Co, and Ni as catalysts. However, due to the Ostwald ripening of metal catalysts, the diameter distribution of the grown SWCNTs is considerably wide (>2 nm), which is not suitable for electronics applications. In addition, reduction in the growth temperature is desirable for fabricating SWCNT devices compatible with the LSI process. Herein, we performed SWCNT growth by alcohol catalytic CVD using platinum-group metal catalysts (Pt, Rh, and Pd) because these metals have high melting points, and the reduction in the Ostwald ripening of catalyst particles is expected. Our results revealed that web-like SWCNTs were obtained from Pt and Rh catalysts at growth temperature between 500 °C and 600 °C by optimizing the ethanol pressure. The SWCNT yield from Pd catalysts was considerably low. By decreasing the growth temperature, the diameter and chirality distribution of SWCNTs from Pt and Rh catalysts became small and narrow. In particular, the diameters of most SWCNTs grown using Pt catalysts were below 1 nm and their diameter distribution was considerably narrow. On the contrary, SWCNTs can grow from Rh catalysts even at 300 °C by optimizing the growth condition, which is the lowest temperature recorded for SWCNT growth. Our results demonstrated that platinum-group metals are useful for the growth of small-diameter SWCNTs and facilitate low-temperature growth.

***Keywords*—**Carbon nanotube, chemical vapor deposition, catalyst, Pt, Rh, Pd.

I. Introduction

SWCNTs [1] are one-dimensional materials with unique properties [2], [3] and have various potentials for future nanoelectronics applications [4-6]. SWCNTs exhibit a number of properties, including ballistic transport [7], high mobility [8], and high current-carrying density (~10^9 A/cm^2) [9], so they have a huge potential in electronics applications, including field-effect transistors (FET) [10], [11], LSI interconnects [12], [13], and energy conversion devices [14], [15]. Because the electronic and optical properties of SWCNTs strongly depend on their chirality [2], the selective growth of SWCNTs having uniform chirality and diameter is one of the most important issues in this field. To date, the most versatile techniques for synthesizing SWCNTs are based on catalyst-assisted CVD. In these techniques, metal-based nanoparticles serve as catalysts in both assisting carbon feedstock cracking and facilitating the nucleation of SWCNTs. In general, transition metal catalysts, including Fe [16], [17], Co [18], [19], and Ni [20], are widely used for SWCNT growth via CVD because of both high efficient production and wide growth windows. However, the chirality of SWCNTs grown using these catalysts is distributed to some extent. Additionally, their diameters are distributed between approximately 1 and 3 nm because of the enlargement of catalyst particles caused by surface migration and/or Ostwald ripening at the growth temperature. To avoid this problem, various bimetal catalysts are used, and SWCNTs having narrow diameter distributions are obtained [21], [22]. However, it is desirable to grow SWCNTs having narrow diameter distributions using only one metal for the simplicity of growth process.

Recently, several groups have attempted SWCNT growth using noble metals as catalysts. Ghorannevis et al. demonstrated SWCNT growth having a narrow chirality distribution from Au catalysts using a plasma CVD method [23]. By controlling the H_2 concentration in CH_4, they demonstrated selective growth of (6,5) SWCNTs. Lie et al. reported that the addition of Pt into Co catalysts in alcohol CVD growth dramatically reduced the diameters of SWCNTs and narrowed their chirality distributions [24]. These results suggest that nanoscale noble metals might have some advantages in the growth of SWCNTs having uniform chirality and diameter.

Herein, we focused on platinum-group metals as catalysts for SWCNT growth. Compared with Fe, Co, and Ni, many platinum-group metals have high melting points, which could suppress the aggregation of catalysts, leading to narrow diameter distributions. We conducted SWCNT growth using the Rh, Pt, and Pd catalysts under various growth conditions via a cold-wall ultrahigh vacuum (UHV) CVD system. Rh and Pt have 8 and 9 *d*-electrons ($4d^8$ and $5d^9$), respectively, which are suitable for SWCNT growth [25]. On the contrary, Pd has 10 *d*-electrons ($4d^{10}$), which is considered to exhibit low activity against feedstock gas containing carbon atoms. We conducted SWCNT growth using these three metals as catalysts and

Takahiro Maruyama is with the Nanomaterials Research Center and the department of Applied Chemistry, Meijo University, Nagoya 468-8502, Japan (corresponding author, phone: +81-52-838-2386; fax: +81-52-832-1179; e-mail: takamaru@meijo-u.ac.jp).

Takahiro Saida is with the Nanomaterials Research Center and the department of Applied Chemistry, Meijo University, Nagoya 468-8502, Japan (e-mail: tsai@meijo-u.ac.jp).

Shigeya Naritsuka is with the Department of Materials Science and Engineering, Meijo University, Nagoya 468-8502, Japan (e-mail: narit@meijo-u.ac.jp).

Sumio Iijima is with the Nanomaterials Research Center and the faculty of Science and Technology, Meijo University, Nagoya 468-8502, Japan (e-mail: tsai@meijo-u.ac.jp).

compared the differences in SWCNT growths.

II. Experimental Procedure

Pt catalysts were deposited on SiO_2(100 nm)/Si substrates using a pulsed arc plasma gun. Rh catalysts were deposited on Al_2O_3 (10 nm)/SiO_2 (100 nm)/Si substrates using electron beam evaporation because SWCNT yields were enhanced by the deposition of Rh catalysts on Al_2O_3 support layers. In the case of Pd catalysts, Al_2O_3 (0.2 nm)/Pd/Al_2O_3 (4 nm)/SiO_2 (100 nm)/Si structures were used for SWCNT growth because the amount of grown SWCNTs was considerably low from Pd on the SiO_2/Si and Al_2O_3/SiO_2/Si substrates.

During SWCNT growth, only ethanol gas was supplied without any carrier gas. The ethanol pressure was monitored using an ion gage on the inside wall of the UHV chamber. The ethanol pressure in this study was much smaller than that at the catalysts on the substrates. During heating, the substrate temperature was monitored using a pyrometer, which can measure the sample temperature between 200 °C and 2000 °C.

SWCNT growth was conducted in a UHV chamber equipped with a stainless-steel nozzle for introduction of the ethanol gas. The details of the equipment used for SWCNT growth are available shown in previous research [26], [27]. Before SWCNT growth, the base pressure was below 1×10^{-6} Pa. The substrate temperature was increased to the growth temperature under H_2 gas flow at a pressure of 1×10^{-3} Pa to prevent the oxidation of the catalysts. The growth time was 1 h for all samples.

The samples were characterized using a field-emission scanning electron microscope (SEM; JSM-6700F, JEOL) and Raman spectroscopy (inVia Reflex, Renishaw). High-resolution transmission electron microscope (TEM, JEM-3100) images were obtained at an accelerating voltage of 200 kV. The TEM samples were prepared using SiO_2 membrane TEM grids to investigate the catalyst particle size.

III. Results and Discussion

A. SWCNTs Grown Using Pt Catalysts

Figs. 1 (a)-(e) show the SEM images of the samples grown using Pt catalysts on SiO_2/Si substrates at a growth temperature between 400 °C and 700 °C. The ethanol pressures used for the growth of these samples were 1×10^{-5} Pa for 400 °C, 450 °C, 500 °C, and 600 °C and 1×10^{-3} Pa for 700 °C. These ethanol pressures were optimized to maximize the SWCNT yield for each growth temperature. Fibrous structures were observed between 500 °C and 700 °C, and their densities increased as the growth temperature increased. However, only a small amount of products was observed at 400 °C and 450 °C. Fig. 1 (f) shows a TEM image of a sample grown at 700 °C under an ethanol pressure of 1×10^{-3} Pa. Several SWCNT bundles were observed, accompanied by Pt particles (black particles in the image), indicating that SWCNTs were grown using Pt catalysts. Fig. 1 (f) also shows that the diameters of most SWCNTs contained in the bundle were below 2 nm. Moreover, some SWCNTs had diameters less than 1 nm.

Figs. 2 (a) and (b) show the Raman spectra of the samples grown using Pt catalysts on SiO_2/Si substrates between 400 °C and 700 °C under the optimal ethanol pressures. The excitation wavelength used for Raman measurements was 785 nm. The Raman spectra of these samples exhibited both G band peaks at 1594 cm^{-1} and radial-breathing-mode (RBM) peaks, indicating that SWCNTs were grown in this temperature range. At a growth temperature of 700 °C, the intensity ratio of G band to D band in the Raman spectrum (G/D ratio) was ~4. When the growth temperature was reduced to 400 °C, the G band intensity decreased, indicating the reduction in the SWCNT yield. In addition, G band became broad and G/D ratio became less than 1. This result demonstrated that the crystallinity of SWCNTs deteriorated as the growth temperature was reduced.

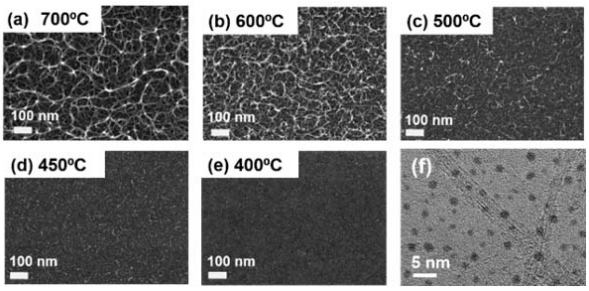

Fig. 1 (a)–(e) Scanning electron microscope (SEM) images of the samples grown using Pt catalysts on SiO_2/Si substrates at growth temperatures of 700 °C, 600°C, 500 °C, 450 °C, and 400 °C, respectively. (f) Transmission electron microscope (TEM) image of a sample grown at 700 °C using Pt catalysts. The ethanol pressures were optimized for each growth temperature to obtain the maximum yield of SWCNTs

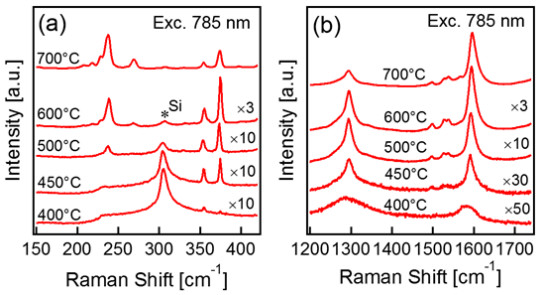

Fig. 2 Raman spectra of (a) the radial-breathing-mode (RBM) region and (b) the high-energy region for SWCNTs grown on SiO_2/Si substrates between 400 °C and 700 ºC using Pt catalysts. The ethanol pressures were optimized for each growth temperature. All spectra were measured at an excitation wavelength of 785 nm

In general, the Raman shift of an RBM peak is related to the SWCNT diameter. The relation between the Raman shift of an RBM peak and the SWCNT diameter is well known, i.e., d (nm) = 248/ω cm^{-1}, where d is the diameter of the SWCNT and ω is the Raman shift [28]. Thus, RBM peaks shown in Fig. 2 (a), which were distributed between 375 and 175 cm^{-1} at a growth temperature of 700 °C, correspond to SWCNTs having diameters between 0.66 and 1.4 nm. On the contrary, when the growth temperature was less than 450 °C, the RBM peaks were distributed between 250 and 375 cm^{-1}, which corresponded to

diameters in the range 0.66–0.69 nm. Both SWCNT diameters and their diameter distributions thus became small and narrow, respectively, as the growth temperature was reduced.

B. SWCNTs Grown Using Rh Catalysts

Figs. 3 (a)–(c) show the SEM images of samples grown using Rh catalysts on $Al_2O_3/SiO_2/Si$ substrates at 600 °C, 500 °C, and 400 °C, respectively. The ethanol pressures used for the growth of these samples were 1×10^{-3}, 1×10^{-4}, and 1×10^{-5} Pa, respectively, which were optimized to maximize the SWCNT yield. When the growth temperature was 600 °C, fibrous structures were observed, which formed a web-like structure. However, the density of these structures was fairly reduced at 500 °C. At 400 °C, only a small amount of products was observed. Fig. 3 (d) shows the TEM image of a sample grown using Rh catalysts at 600 °C under an ethanol pressure of 10^{-3} Pa. In addition, SWCNTs were observed, accompanied by Rh particles (black particles in the image). This result also indicates that SWCNTs were grown using Rh catalysts.

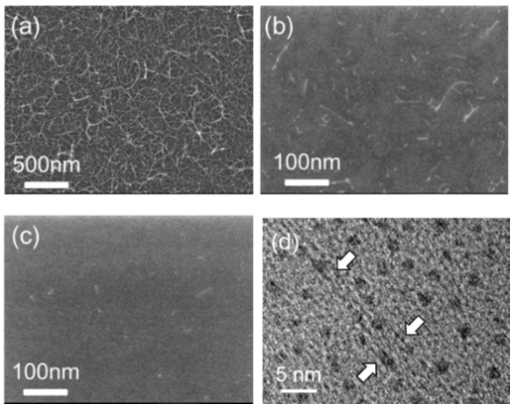

Fig. 3 (a)–(c) SEM images of the samples grown using Rh catalysts on $Al_2O_3/SiO_2/Si$ substrates at growth temperatures of 600 °C, 500 °C, and 400 °C, respectively. (d) TEM image of a sample grown at 600 °C using Rh catalysts. The ethanol pressures were optimized for each growth temperature to obtain the maximum yield of SWCNTs

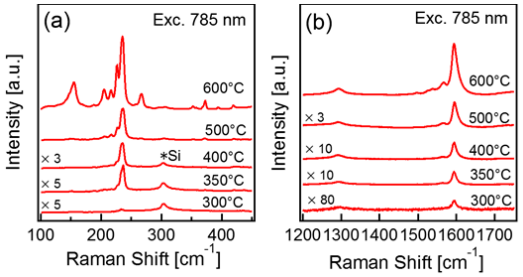

Fig. 4 Raman spectra of (a) the RBM region and (b) the high-energy region for SWCNTs grown on $Al_2O_3/SiO_2/Si$ substrates between 300 °C and 600 °C using Rh catalysts. The ethanol pressures were optimized for each growth temperature. All spectra were measured at an excitation wavelength of 785 nm

Figs. 4 (a) and (b) show the Raman spectra of the samples grown using Rh catalysts on $Al_2O_3/SiO_2/Si$ substrates between 300 °C and 600 °C under the optimal ethanol pressures. The excitation wavelength was 785 nm. The Raman spectra exhibited both G band peaks and RBM peaks, indicating that SWCNTs were grown in this temperature range. The G/D ratio decreased with a decrease in the growth temperature, which was ~4 even at 400 °C. In addition, the full width at half maximum (FWHM) of G band in the Raman spectra of SWCNTs grown using Rh catalysts was narrower than SWCNTs grown using Pt catalysts at a growth temperature of 400 °C. This result shows that both the yield and crystalline quality of SWCNTs grown using Rh catalysts were better than those of SWCNTs grown using Pt catalysts. Additionally, Rh catalysts were suitable for SWCNT growth at low temperatures. In addition, the diameter distribution became narrow as the growth temperature was reduced. It should be noted that both a G band peak and an RBM peak appeared at 1594 and 240 cm^{-1}, respectively, even at a growth temperature of 300 °C. This result indicates that SWCNTs were grown using Rh catalysts even at such a low temperature.

C. SWCNT Grown Using Pd Catalysts

Figs. 5 (a) and (b) show the SEM images of the samples grown using Pd catalysts in $Al_2O_3/Pd/Al_2O_3/SiO_2/Si$ substrates at 600 °C and 500 °C, respectively. The optimized ethanol pressure used for the growth of both samples was 1×10^{-4} Pa. At both temperatures, only a few fibrous structures were observed on the substrates. Figs. 5 (c) and (d) show the Raman spectra of the samples at 600 °C and 500 °C, respectively. The excitation wavelength used for the Raman measurements was 633 nm. Both the G band (at 1594 cm^{-1}) and distinct RBM peaks were observed at 141 cm^{-1} for both growth temperatures, indicating that SWCNTs were grown using Pd catalysts. The G/D ratio was greater than 10, indicating that the crystalline quality of SWCNTs was considerably good. However, SEM images revealed that the amount of SWCNTs grown using Pd catalysts was considerably lower than the amount of SWCNTs grown using the Pt and Rh catalysts. Thus, Pd catalysts are not suitable for SWCNT growth at low temperatures.

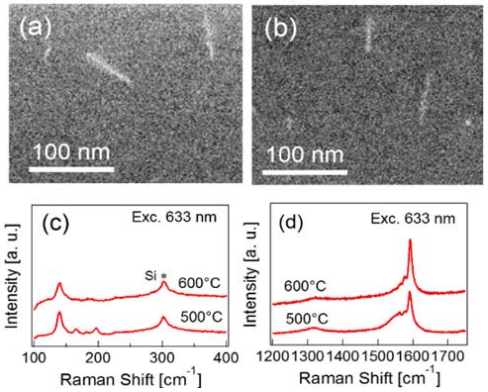

Fig. 5 (a) and (b) SEM images and (c) and (d) Raman spectra of the samples grown using Pd catalysts on $Al_2O_3/Pd/Al_2O_3/SiO_2/Si$ substrates. (a) and (b) SEM images at growth temperatures of 600 °C and 500 °C, respectively. Raman spectra of (c) the RBM region and (d) the high-energy region, which were measured at an excitation wavelength of 633 nm

D.Comparison between the Pt and Rh Catalysts

In the previous section, we showed that Pt and Rh catalysts were suitable for SWCNT growth at growth temperatures below 600 °C. Therefore, in this section, we compared these two catalysts with regard to SWCNT growth. In our samples, SWCNTs wither formed web-like structures or were sparsely grown on the substrates. Therefore, the intensity ratio of the G band peak to the Si peak at ~520 cm^{-1} (G/Si intensity ratio) in the Raman spectra roughly corresponded to the SWCNT yield. Fig. 6 shows a plot of G/Si intensity ratio versus the growth temperature for SWCNTs grown using the Rh and Pt catalysts. The samples used for this plot were grown under the optimal ethanol pressures, so the SWCNT yields were maximized at each growth temperature. For both catalysts, the G/Si intensity ratio decreased as the growth temperature was reduced, indicating that the SWCNT yield decreased as the growth temperature decreased, as stated in previous sections. It is worth noting that the G/Si intensity ratio for Rh catalysts was similar to or stronger than that for Pt catalysts, regardless of the growth temperature. Therefore, among these two catalysts, Rh was found to be effective and suitable for SWCNT growth at low temperatures.

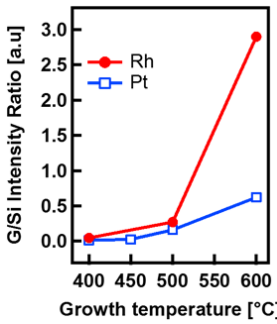

Fig. 6 The relation between the intensity ratio of the G band peak to the Si peak at ~520 cm^{-1} of SWCNTs grown using the Pt and Rh catalysts and the growth temperature. The ethanol pressures used for SWCNT growth were optimized at each temperature to maximize the SWCNT yield

To compare the structural properties of SWCNTs grown from these two catalysts, we performed Raman measurements for SWCNTs grown using the Pt and Rh catalysts at 400 °C by employing lasers at four excitation wavelengths (488, 532, 633, and 785 nm) because the RBM peak was found to have strongly enhanced under the resonance condition wherein the incident laser energy coincided with an electronic transition energy in the SWCNT. Fig. 7 shows the RBM regions of the Raman spectra of SWCNTs grown using the Pt and Rh catalysts at 400 °C under the optimal ethanol pressures. For the samples grown using Pt catalysts, RBM peaks were observed in the Raman spectra measured using only 633- and 785-nm lasers [Figs. 7 (c) and (d)]. In the Raman spectrum using the 633-nm laser [Fig. 7 (c)], weak RBM peaks were observed at 251, 283 and 351 cm^{-1}, while relatively strong RBM peaks appeared at 349 and 369 cm^{-1} in Raman spectrum measured using the 785-nm laser (Fig. 7 (d)). These results revealed that the diameters of SWCNTs grown using Pt catalysts were mainly distributed between 0.67 and 0.99 nm. In the other words, the diameters of SWCNTs grown using Pt catalysts were relatively small and their distribution was narrow. As for Rh catalysts, RBM peaks were observed in Raman spectra for all excitation wavelengths. In particular, strong RBM peaks appeared at 196 and 235 cm^{-1} in the Raman spectra measured using 633- and 785-nm lasers, respectively. In addition, the Raman spectra measured using 488-, 532-, and 633-nm lasers exhibited that weak RBM peaks were distributed between 172 and 282 cm^{-1}. This indicates that the diameters of SWCNTs grown using Rh catalysts were distributed in the range 0.88–1.44 nm. Compared with the Pt and Rh catalysts in the low-temperature growth, SWCNTs grown using Pt catalysts exhibited small diameters and narrow diameter distribution, while the SWCNT yield obtained using Rh catalysts was higher than that obtained using Pt catalysts.

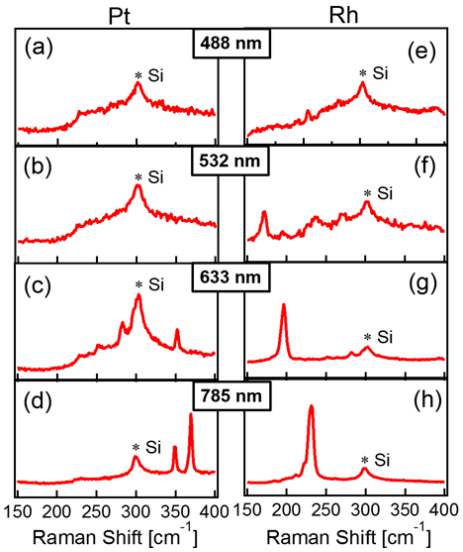

Fig. 7 Raman spectra of the RBM regions for SWCNTs grown at 400 °C under an ethanol pressure of 1×10^{-5} Pa using (a)–(d) Pt catalysts and (e–h) Rh catalysts. The Raman spectra were measured using lasers at four excitation wavelengths: 488 (a) and (e), 532 (b) and (f), 633 (c) and (g), and 785 nm (d) and (f)

Previously, Vesselli et al. reported that the dissociation barrier of the C–C bond of an ethanol molecule on the Rh(111) surface was only 0.6 eV [29]. Later, a study employing density functional theory (DFT) also showed that the maximum activation energy was ~1.0 eV in the dissociation route of ethanol molecules on the Rh(111) surface, which is smaller than that on other transition metal surfaces [30]. From these simulations, we found that the dissociation of an ethanol molecule could easily occur on the Rh surface, thereby enhancing SWCNT growth at low temperatures. As for the SWCNT diameter, it is considered that the SWCNT diameter decreases as the catalyst particle size decreases [31], [32]. However, our TEM observation revealed that catalyst particle sizes were similar between the Pt and Rh catalysts; however, the diameters of SWCNTs grown using Pt catalysts were much smaller than those of SWCNTs grown using Rh catalysts. At

present, the reason for this phenomenon is unclear. There is a possibility that the nucleation mechanism of carbon nanocaps at the catalyst particles is different between the Pt and Rh catalysts.

IV. Conclusion

SWCNT growth was conducted via alcohol catalytic CVD using the Pt, Rh, and Pd catalysts. Compared with the Pt and Rh catalysts, the SWCNT yield from Pd catalysts was considerably low. On the contrary, SWCNTs were grown using the Pt and Rh catalysts at growth temperatures between 400 °C and 700 °C. In particular, by optimizing the ethanol pressure, SWCNTs were grown using Rh catalyst even at 300 °C. Furthermore, SWCNTs grown using Pt catalysts had small diameters and exhibited narrow diameter distributions. We demonstrated that the Pt and Rh catalysts are useful catalysts for SWCNT growth.

Acknowledgment

This research was partially supported by the Program for the Strategic Research Foundation at Private Universities and the Meijo University Research Branding Project, which was supported by the Ministry of Education, Culture, Sports, Science and Technology (MEXT), Japan. Part of this research was conducted at the Institute for Molecular Science (IMS), supported by the "Nanotechnology Platform" of MEXT, Japan. We thank Dr. Nakao of IMS for providing the SEM facility.

References

[1] S. Iijima, and T. Ichihashi, "Single-shell carbon nanotubes of 1-nm diameter," Nature, vol. 363, pp. 603-605, 1993.
[2] R. Saito, G. Dresslehaus, and M. S. Dresselhaus, "Physical Properties of Carbon Nanotubes," Imperial College Press, London, 1998.
[3] M. Meyyappan, "Carbon Nanotubes: Science and Applications," CRC Press, FL; Boca Raton, 2005.
[4] S. J. Trans, M. H. Devoret, H. J. Dai, A. Thess, R. E. Smalley, L. J. Geerligs, and C. Deller, "Individual single-wall carbon nanotubes as quantum wires," Nature, vol. 386, pp.474-477, 1997.
[5] J. Robertson, G. Zhong, S. Hofmann, B. C. Bayer, C. S. Esconjauregui, H. Telg, and C. Thomsen, "Use of carbon nanotubes for VLSI interconnects," Diam. Relat. Mater., vol. 18, pp. 957-962, 2009
[6] J. Chen, V. Perebeinos, M. Freitag, J. Tsang, Q. Fu, J. Liu, and P. Avouris, "Bright infrared emission from electrically induced excitons in carbon nanotubes," Science, vol. 310, pp. 1171-1174, 2005.
[7] A. Javey, J. Guo, Q. Wang, M. Lundstrom, and H. Dai, "Ballistic carbon nanotube field-effect transistors," Nature, vol. 424, pp. 654-657, 2003.
[8] T. Dürkop, S. A. Getty, E. Cobas, and M. S. Fuhrer, "Extraordinary mobility in semiconducting carbon nanotubes," Nano Lett., vol. 4, pp. 35-39, 2004.
[9] S. Hong, and S. Myung, "Nanotube electronics: a flexible approach to mobility," Nat. Nanotech., vol. 2, pp. 207-208, 2007.
[10] S. J. Tans, A. R. M. Vershueren, and C. Dekker, "Room-temperature transistor based on a single carbon nanotube," Nature, vol. 393, pp. 49-52, 1998.
[11] S. J. Wind, J. Appenzeller, R. Martel, V. Derycke, and P. Avouris, "Vertical scaling of carbon nanotube field-effect transistors using top gate electronics," Appl. Phys. Lett., vol. 80, pp. 3817-3819, 2002.
[12] D. Kondo, S. Sato, A. Kawarada, and Y. Awano, "Selective growth of vertically aligned double- and single-walled carbon nanotubes on a substrate at 590°C," Nanotechnol., vol. 19, pp. 435601, 2008.
[13] T. Iwasaki, J. Robertson, and H. Kawarada, "Mechanism analysis of interrupted growth of single-walled carbon nanotube arrays," Nano Lett., vol. 8, pp. 886-890, 2008.
[14] G. Girishkumar, K. Vinodgopal, and P. V. Kamat, "Carbon nanostructure in portable fuel cells: single-walled carbon nanotube electrodes for methanol oxidation and oxygen reduction," J. Phys. Chem. B, vol. 108, pp. 19960-19966, 2004.
[15] M. W. Rowell, M. A. Topinka, M. D. McGehee, H.-J. Prall, G. Dennler, N. S. Sariciftci, L. Hu, and G. Gruner, "Organic solar cells with carbon nanotube network electrodes," Appl. Phys. Lett., vol. 88, pp. 233506, 2006.
[16] K. Hata, D. N. Futaba, K. Mizuno, T. Namai, M. Yumura, and S. Iijima, "Water-assisted highly efficient synthesis of impurity-free single-walled carbon nanotube," Science, vol. 306, pp. 1362-1364, 2004.
[17] G. Zhong, T. Iwasaki, J. Robertson, and H. Kawarada, "Growth kinetics of 0.5 cm vertically aligned single-walled carbon nanotubes," J. Phys. Chem. B, vol. 111, pp. 1907-1910, 2007.
[18] S. Maruyama, R. Kojima, Y. Miyauchi, S. Chiashi, and M. Kouhno, "Low-temperature synthesis of high-purity single-walled carbon nanotubes from alcohol," Chem. Phys. Lett., vol. 360, pp. 229-234, 2002.
[19] M. Fouquet, B. C. Bayer, S. Esconjauregui, R. Blume, J. H. Warner, S. Hofmann, R. Schlögl, C. Thomsen, and J. Robertson, "Highly chiral-selective growth of single-walled carbon nanotubes with a simple monometallic Co catalysts," Phys. Rev. B, vol. 85, pp. 235411, 2002.
[20] M. Paillet, V. Jourdain, P. Poncharal, J.-L. Sauvajol, and A. Zahab, "Versatile synthesis of individual single-walled carbon nanotubes from nickel nanoparticles for the study of their physical properties," J. Phys. Chem. B, vol. 108, pp. 17112-17118, 2004.
[21] E. Mora, J. M. Pigos, F. Ding, B. I. Yakobson, and A. R. Harutyunyan, "Low-temperature single-wall carbon nanotubes synthesis: Feedstock decomposition limited growth," J. Am. Chem. Soc., vol. 130, pp. 11840-11841, 2008.
[22] B. Wang, C. H. Patrick Poa, L. Wei, L.-J. Li, Y. Yang, and Y. Chen, "(n, m) selectivity of single-walled carbon nanotubes by different carbon precursors on Co-Mo catalysts," J. Am. Chem. Soc., vol. 129, pp. 9014-9019, 2007.
[23] Z. Ghorannevis, T. Kato, Y. Kaneko, and R. Hatakeyama, "Narrow-chirality distributed single-walled carbon nanotube growth from nonmagnetic catalyst," J. Am. Chem. Soc., vol. 132, pp. 9570-9572, 2010.
[24] B. Lie, W. Ren, S. Li, C. Liu, and H.-M. Cheng, "High temperature selective growth of single-walled carbon nanotubes with a narrow chirality distribution from a CoPt bimetallic catalyst," Chem. Commun., vol. 48, pp. 2409-2411, 2012.
[25] T. Maruyama, "Current status of single-walled carbon nanotube synthesis from metal catalysts by chemical vapor deposition," Mater. Express, vol. 8, pp. 1-20, 2018.
[26] T. Maruyama, H. Kondo, R. Ghosh, A. Kozawa, S. Naritsuka, Y. Iizumi, T. Okazaki, and S. Iijima, "Single-walled carbon nanotube synthesis using Pt catalysts under low ethanol pressure via cold-wall chemical vapor deposition in high vacuum," Carbon, vol. 96, pp. 6-13, 2016.
[27] T. Maruyama, A. Kozawa, T. Saida, S. Naritsuka, and S. Iijima, "Low temperature growth of single-walled carbon nanotubes from Rh catalysts," Carbon, vol. 116, pp. 128-132, 2017.
[28] A. Jorio, R. Saito, J. H. Hafner, C. M. Liever, M. Hunter, T. McClure, G. Dresselhaus, and M. S. Dresselhaus, "Structural (n, m) determination of isolated single-wall carbon nanotubes by resonant Raman scattering," Phys. Rev. B, vol. 86, pp. 1118-1121, 2001.
[29] E. Vesselli, A. Baraldi, G. Comelli, S. Lizzit, and R. Rosei, "Ethanol decomposition: C-C cleavage selectivity on Rh(111)," ChemPhysChem, vol. 5, pp. 1133-1140, 2004.
[30] J. H. Wang, C. S. Lee, M. C. Lin, "Mechanism of ethanol reforming: theoretical foundations," J. Phys. Chem. C, vol. 113, pp. 6681-6688, 2009.
[31] C. L. Cheung, A. Kurtz, H. Park, and C. M. Liever, "Diameter-controlled synthesis of carbon nanotubes," J. Phys. Chem. B, vol. 106, pp. 2429-2433, 2002.
[32] M. Paillet, V. Joudain, P. Poncharal, J.-L. Sauvajol, and A. Zahab, "Versatile synthesis of individual single-walled carbon nanotubes from nickel nanoparticles for the study of their physical properties," J. Phys. Chem. B, vol. 108, pp. 17112-17118, 2004.